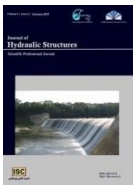
Journal of Hydraulic Structures
J. Hydraul. Struct., 2021; 7(1):16-37
DOI: 10.22055/jhs.2021.37091.1167



Estimation of Parameters in Groundwater Modeling by Particle Filter linked to the meshless local Petrov-Galerkin Numerical Method

Ali Mohtashami [1]
Seyed Arman Hashemi Monfared [2]
Gholamreza Azizyan [3]
Abolfazl Akbarpour [4]

Abstract

The present study employs a mathematical method, i.e., Particle Filter (PF), to accurately estimate the parameters of three standard aquifers. The method is linked to a new developed numerical method, i.e., meshless local Petrov-Galerkin based on the moving kriging method (PF-MLPG-MK), to determine the aquifer parameters such as hydraulic conductivity coefficient, transmissivity coefficient, and storage coefficient or specific yield appropriately. For this purpose, a set of particles scattered in the state space. Each particle has two features: location and weight. Particles with greater weight values have the closer location to the estimation. Weight values which are assigned to each particle is computed based on the maximum likelihood function. This function is calculated in MLPG-MK simulation model. Overall, by linking particle filter model to the accurate simulation model, an efficient estimation method for aquifer parameters is obtained. This model applied to three standard aquifers. In the first standard aquifer, the estimated parameters of hydraulic conductivity and specific yield were 30.21 and 0.143, respectively. However, the exact values are 30 and 0.15. Also, in the second standard aquifer, the predicted transmissivity and storage coefficients were 99.7038 and 0.001057 whereas their true values are 100 and 0.001. In the third aquifer, the exact value of six parameters were achieved. The sensitivity analysis of the number of particles was carried out. Results revealed that with increasing the particles more accuracy will be achieved. 60, 80 and 100 particles were considered in the model. Results for 100 particles showed more accuracy.

Keywords: Aquifer Hydrodynamic Parameters, Groundwater Modelling, Particle Filter, Meshless Local Petrov-Galerkin.

Received: 10 April 2021; Accepted: 25 May 2021

[1] Department of Civil Engineering, Faculty of Engineering, University of Sistan and Baluchestan, Zahedan, Iran, E-mail: mohtashamiali@pgs.usb.ac.ir
[2] Department of Civil Engineering, Faculty of Engineering, University of Sistan and Baluchestan, Zahedan, Iran, E-mail: hashemi@eng.usb.ac.ir **(Corresponding Author)**
[3] Department of Civil Engineering, Faculty of Engineering, University of Sistan and Baluchestan, Zahedan, Iran, E-mail: G.azizyan@eng.usb.ac.ir
[4] Department of Civil Engineering, Faculty of Engineering, University of Birjand, Birjand, Iran, E-mail: akbarpour@birjand.ac.ir

1. Introduction

Groundwater is one of the main sources of fresh water in all regions and the only source of water supply in arid and semi-arid regions of the world. Even in countries with favorable rainfall conditions, groundwater is still considered the primary source due to easy access [1]. Nowadays, the expansion of groundwater exploitation has caused a dramatic drawdown in groundwater levels [2]. The overwhelming extraction of groundwater, occurring due to population growth and the rapid development of urbanization and also new industries, has been rapidly depleted these resources. Therefore, the sound management of these resources is essential. This is one of the main strategies adopted by engineers and water managers to alleviate the damage impacts on the aquifer by which they can advance their goals for decision making and planning of water consumption [3],[4].

Groundwater models are generally used to manage these resources as a helpful tool. These models solve the partial differential equations of a groundwater system for which data on hydrogeology of the study zone is required. Since aquifers are anisotropic, the parameters are not distributed across them uniformly. Therefore, efficient groundwater management is dependent on providing accurate data on transmissivity coefficient, hydraulic conductivity, and specific yield [5]. Solicitation of such data to anticipate groundwater levels in a specific zone is an essential problem. Since these parameters vary across an aquifer due to the spatial distribution of the aquifer, hydrogeologist can hardly gather sufficient information about them at different spots of an aquifer. It should be noted that providing precise information on these parameters in a large aquifer is time-consuming and costly. Accordingly, it is required to find a way to determine the values of these parameters most accurately but with the lowest possible cost and in the shortest possible time.

The present paper employs the particle filtering approach to estimate the aquifer parameters. In engineering processes, real time and reliable estimation of a dynamic system is a key element in model-based approaches, such as optimizations, simulations, and monitoring systems [6]. The main idea behind the particle filter is to estimate the probability density function due to the production of a large number of samples (particles), each of which has its own weight. These particles and their weights are updated sequentially by following the new observational data available [7]. This model, which is a real time model, is used to find the optimal and correct values of the parameters compared to the observed values at different locations and times across the study zone. The transmissivity coefficient, hydraulic conductivity coefficient, storage coefficient, and also specific yield are often the most significant calibration parameters in aquifers. Furthermore, other parameters, such as the extraction of wells, recharge value, and boundary conditions can be considered for the calibration process [8]. The particle filtering technique is used to allocate appropriate values to the model parameters, thereby predicting the parameters to the extent that the best match is achieved by comparing the model outputs with the field data. In the simulation process of the groundwater flow, model outputs can be several variables, such as hydraulic head and groundwater drawdown.

In recent years, several studies have been conducted on aquifer parameters [9-15]. For instance, Carrera et al. [16] discussed all the factors influencing aquifer parameters, uncertainties, and different parameter estimation models.

Hill [17] presented a simplified model to calculate aquifer parameters. The main advantage of that model was that it could be applied to all aquifers under any conditions. They also stated that although this model was developed for groundwater, it was applicable to all engineering fields.

Fu & Gómez-Hernández [18] pointed out that groundwater and mass transfer contained

highly uncertain parameters. Then, using the Markov Chain based on the Monte Carlo uncertainty method, they estimated the parameters for an assumed aquifer and anticipated them for places where sampling was not possible. Ayvaz et al. [19] used observational data on the water surface to propose an inverse modeling algorithm in order to zone and determine the parameters of an aquifer. It is worth noting that Ayvaz et al. [19] used a kernel-based fuzzy c-means (KFCM) approach for the aim of zonation. Their model does not require an initial estimation. They implemented their algorithm on two test cases and then performed a sensitivity analysis on their work. The results stated that the utilized algorithm was efficient and effective in determining aquifer parameters and zonation. Copty et al. [20] computed parameters of a confined aquifer at any point in time using an approach based on the ratio of the drawdown to the logarithmic derivative of drawdown. Sahin [21] used a new approach based on the radial basis function collocation method to estimate confined aquifer parameters. The performance of his approach examined under several pump tests scheme in different test cases involved isotropic and anisotropic conditions. Lastly, He compared his results with ANN[5] estimation method. Results determined that his approach was as viable alternative technique for estimation. Swathi and Eldho [22] used a simulation-optimization (SO) model in order to determine the aquifer parameters and zonation structures. Their SO model comprised MLPG numerical method and particle swarm optimization algorithm. A hypothetical aquifer case study was engaged as well. Weighted least square approach was applied for inverse modelling aims. They found the proposed method effective and satisfactory even in real field aquifer. Naderi [23] estimated parameters of three confined aquifers using simple derivative-based method. He applied his method for a synthetic, published and a real aquifer. Transmissivity, hydraulic conductivity and storage coefficients were the estimated parameters. His results showed that the estimation accuracy was satisfactory and acceptable. Thomas et al. [24] presented a new SO model by linking radial point collocation method (RPCM) and cat swarm optimization (CSO) for estimation of aquifer parameters. They applied their model in two aquifers, one is standard and the other one is regional. Achieved results showed the reliable performance of RPCM and CSO as estimation method.

Thomas et al. [25] developed a simulation-optimization model in order to simulate contaminant transport process and estimate the parameters of their simulation model. Simulation model was radial point collocation method which is recognized as the strong form of finite element methods. Also, cat swarm optimization and particle swarm optimization were engaged to estimate transmissivity, longitudinal dispersion and transverse dispersion. Eryiğit [26] used modified clonal selection algorithm as optimization method to estimate four groundwater flow parameters. MODLFOW was engaged as simulator as well. the proposed model was applied in two hypothetical cases. Results presented the feasibility of the model in estimation of groundwater parameters.

A few studies have addressed the use of meshless methods to simulate groundwater flow. Swathi and Eldho [27] employed MLPG to simulate groundwater flow in two hypothetical and one real aquifers. They used radial basis function for construction of shape function. Finally, they compared their results with FDM and FEM solutions. High accuracy of MLPG methods showed it power and capability. Mohtashami et al. [28] developed MLPG model in order to simulate groundwater flow in Birjand unconfined aquifer. Their engaged method was based on the moving least square's function (MLS). They verified MLPG model with FDM solutions. The comparison presented high accuracy of MLPG-MLS model. As the RMSE error for MLPG-

[5] Artificial Neural Network

MLS and FDM was 0.757m and 1.541m respectively. Pathania et al. [29] used meshless method named element free Galerkin (EFG) in order to simulate groundwater flow in three aquifers. They mentioned high accuracy of EFG in comparison of grid-based methods e.g., FDM and FEM.

In this study, particle filter method, one of the robust data assimilation (DA) techniques is used to accurately predict the hydrodynamic parameters of three standard aquifers. This powerful method known as a real time approach is engaged for the first time in this filed. For this aim, particle filter linked to the meshless groundwater simulation model to develop an online calibration/simulation model named PF-MLPG-MK. Meshless local Petrov-Galerkin based on the moving kriging function (MLPG-MK) is the simulation model. Lastly, the proposed model (PF-MLPG-MK) is applied to three standard aquifers for estimation of aquifer parameters.

2. Methods

2.1. Particle filter

A particle filter known as a powerful estimation method computes the probability density function of a random process and also estimates the exact state of the object in the future time based on the states and observations of previous times. The particle filter makes some estimates for the state of the object to select the best one [30].

To this end, in the initial step, particles are scattered in the space which its dimension equals to the number of parameters that must be estimated. The particles are state vectors that are aggregated and use the probability distribution function. Weight values assign to each particle. This weight value in the first step is equal for all particles around $(\frac{1}{N})$ (N is the number of the particles scattered in state space) [30]. In the next step, the weight value depending on the position of the particle is updated. Once the weight of each particle is determined, to prevent from degeneracy occurrence, re-sampling method is carried out.

To be more specific, the particles with very low weight are emitted, and the particles with high weight are involved in the generation of new particles around their coordinates. This function reduces computation time and prevents the particles from spreading in vain [31].

The particle filtering is an effective way to solve the estimation issues in nonlinear Gaussian noise systems. This method is a part of the Monte Carlo statistical methods. In order to describe the particle filter, consider the following nonlinear system:

$$x_t = f(x_{t-1}) + w_{t-1} \quad (1)$$

$$y_t = g(x_t) + v_t \quad (2)$$

where x_t is the state vector, y_t is the measurement vector, and f and g are nonlinear functions, respectively. Furthermore, it is assumed that w_t and v_t are processes called noise and measurement noise, respectively. The particle filter of the posterior probability density function $p(x_t|y_{1:t})$ is defined as a set of weighted particles as follows (Figure 1):

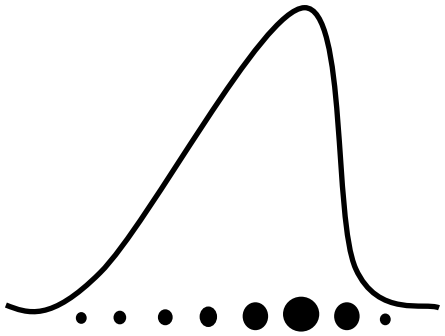


Figure 1. Descriptions of posterior function [32]

$$S_t = \left\{\left(x_t^{(i)}, w_t^{(i)}\right)\middle|\, \mathrm{i} = 1, \dots, \mathrm{N}\right\} \tag{3}$$

where N, $x_t^{(i)}$ and $w_t^{(i)}$ are the number, locations and weights of particles. The particle filter approximates the posterior function of $p(x_t|y_{1:t})$ as follows [32],[33]:

$$p(x_t|y_{1:t}) \sim \sum_{i=1}^{N} w_t^{(i)} \delta(x_t - x_t^{(i)}) \tag{4}$$

where $\delta(x)$ is the Dirac Delta function and $w_t^{(i)} > 0$ is the weight of $x_t^{(i)}$ and $\sum_{i=1}^{N} w_t^{(i)} = 1$.

Direct sampling from the probability density function (known as the objective weighing function) is not possible; hence, the important sampling method is used. In the important sampling method, instead of directly sampling the target function, a proposed weighing function is proposed. Considering the proposed density function as $q(x_{0:t}|y_{1:t})$, the particle weight is calculated as follows [32]:

$$w_t^{(i)} = \frac{p(x_{0:t}^{(i)}|y_{1:t})}{q(x_{0:t}^{(i)}|y_{1:t})} \tag{5}$$

By decomposing the proposed density function as follows, weights will be calculated recursively [34]:

$$q(x_{0:t}|y_{1:t}) = q(x_t|x_{0:t-1}, y_{1:t}) \times q(x_{0:t-1}|y_{1:t-1}) \tag{6}$$

In this case, the particles of $x_{0:k}^{(i)}$ that are a sample from the proposed density distribution function of $q(x_{0:k-1}|y_{1:k-1})$ are obtained by the new state of $x_{0:k}^{(i)}$ that is sampled from $(x_{0:k}|x_{0:k-1}, y_{1:k-1})$. The weight of these particles is as follows [35],[36]:

$$w_t^{(i)} = \frac{p(x_{1:t}|y_{1:t})}{q(x_{t:t-1}|y_{1:t-1}) \times q(x_1|y_t, x_{t-1})} \tag{7}$$

On the other hand, according to the Bayes law, the posterior probability density function can be written as follows [32]:

$$\begin{aligned} p(x_{0:k}|y_{1:k}) &= \frac{p(y_k|x_{0:k}, y_{1:k-1})p(x_{0:k}|y_{1:k-1})}{p(y_k|y_{1:k-1})} = \frac{p(y_k|x_{0:k}, y_{1:k-1})p(x_k|x_{0:k-1}, y_{1:k-1})}{p(y_k|y_{1:k-1})} p(x_{0:k-1}|y_{1:k-1}) \\ &= \frac{p(y_k|x_k)p(x_k|x_{k-1})}{p(y_k|y_{1:k-1})} p(x_{0:k-1}|y_{1:k-1}) \propto p(y_k|x_k, y_{1:k-1})p(x_k|x_{k-1})p(x_{0:k-1}|y_{1:k-1}) \end{aligned} \tag{8}$$

So, the particle weight is calculated as the following recursive relation [33]:

$$w_t^{(i)} = w_{t-1}^{(i)} \frac{p(y_t|x_t^{(i)})p(x_t^{(i)}|x_{t-1}^{(i)})}{q(x_t^{(i)}|x_{t-1}^{(i)}, y_{1:t})} \tag{9}$$

This method is known as the post probability of significant sequential important sampling

(SIS) [32, 33]. In order to avoid the degeneracy phenomenon, which is occurred when the variance values of particles becoming high and their weight values reached to zero and make the estimation to be ill, re-sampling, the sequential important sampling algorithm is introduced [37]. This algorithm which is known as the sequential important re-sampling (SIR) algorithm has three steps including sampling, calculating particle weight, and re-sampling:

1- Sampling: The particles are obtained by sampling from the proposed distribution.
$$x^{(i)} \sim q(x_t|y_{1:t}) \tag{10}$$
2- Calculating particle weight with using Eq. 9.
3- Re-sampling: Higher-weight particles replace the lower-weight particles.

As we mentioned, particle degeneracy occurs in particle filter when the variance of weight values becoming large. This is the main drawback of particle filter. In order to solve this problem, resampling method recommended. In this technique, the following concept introduced in equation 11 [32]:

$$N_{eff} = \frac{1}{\sum_{i=1}^{N} \left(w_t^{(i)}\right)^2} \tag{11}$$

In this equation, when the weight value ($w_t^{(i)}$) is lower than a threshold size (N_{thresh}), resampling algorithm activates. The important issue is the value of (N_{thresh}). Based on the references presented in this field, the best value for this parameter is $\frac{N}{2}$ [38],[39]. The following equation shows the condition that resampling technique must be carried out [38]:

$$if\ N_{eff} < (N_{thresh} = \frac{N}{2}) \rightarrow Resampling\ procedure\ is\ needed \tag{12}$$

Resampling technique makes the particle filter method compatible with the condition of problem and removes the particle degeneracy. In this paper, the particles considered the state space amount to 100, 80 and 60. The different number of particles considered in the PF-MLPG-MK model and sensitivity analysis is carried out.

2.2. Meshless local Petrov-Galerkin (MLPG)

Extensive research has been carried out in fluid mechanics related to the meshless methods. These methods remove the drawbacks of the gird-based numerical methods, e.g., FEM and FDM, with just adding or deleting a set of field nodes [40]. They overcome the limitations of the FEM numerical method in updating boundary conditions [41]. These methods have outperformed FEM in terms of accuracy [42]. Also, the defects of the finite difference method, which is restricted to the rectangular meshes, are eliminated in these numerical methods.

MLPG is a weak form of meshless methods presented in 1998 by Atluri and Zhu [43] to solve the potential equation. This method is generally used in fluid mechanics and involves two functions: the weight function (cubic spline) and moving kriging. The moving kriging function is used to construct a shape function. For more details refer to Mohtashami et al. [28],[44] It should be mentioned that MLPG has already been used by authors to simulate groundwater flow in field aquifer and it is calibrated and verified by the observation data and FDM solutions. The higher

accuracy of MLPG indicates its power and capability [45],[46].

2.3. Moving Kriging method (MK)

Moving kriging method formulation is similar to MLS[6] approximation function which is used by MLPG in order to construct shape function. This function satisfies the Kronecker delta property. consider the function $(h^h(X))$ is defined as groundwater head. Therefore, the formulation of shape function is presented in Eq. 13

$$h^h(X) = \sum_{L}^{n} \phi_L(X) h_I \tag{13}$$

Where $\phi_I(X)$is the shape function and L is the number of nodes scattered in the whole domain. In this equation, $\phi_I(X)$ is computed with the following equation:

$$\phi(x) = p^T(x)A + r^T(x)B \tag{14}$$

Where A and B are expressed as:

$$A = (P^T R^{-1} P)^{-1} P^T R^{-1} \tag{15}$$

$$B = R^{-1}(I - PA) \tag{16}$$

In these equations I is a unit matrix and $P(X)$ is the basis function obtained from the monomials in the Khayyam-Pascal triangle. R and $r(X)$ are defined in Eq. (17) and (18):

$$R = \begin{bmatrix} r(x_1, x_1) & \dots & r(x_1, x_N) \\ \dots & & \dots \\ r(x_N, x_1) & \dots & r(x_N, x_N) \end{bmatrix} \tag{17}$$

$$r^T(x) = [r(x, x_1)\ r(x, x_2) \dots\ r(x, x_N)] \tag{18}$$

Where $r(x_i, x_j)$ is the correlation function between any pair of nodes located at x_i and x_j.

2.4. Groundwater flow equation in the confined aquifer

The governed equation for groundwater flow in a transient condition is given in Eq. 19 [47]:

$$k_x \frac{\partial}{\partial x}\left(\frac{\partial H}{\partial x}\right) + k_y \frac{\partial}{\partial y}\left(\frac{\partial H}{\partial y}\right) = S\frac{\partial H}{\partial t} + Q \times \delta(x - x_w)(y - y_w) + q \tag{19}$$

where the initial condition is considered with the results achieved from the steady condition [47]. The boundary condition in groundwater studies can be defined as the constant head boundary (Dirichlet), constant flow boundary (Neumann) [46]. Here, H represents groundwater head [L], k stands for hydraulic conductivity coefficient [L/T], Q denotes the discharge (+) or recharge (-) rate [L/T], δ is the Dirac delta function, S is storage coefficient, and q stands for the distributed flow, e.g., precipitation and evaporation.

After the discretization of the groundwater flow equation, a set of linear equations are generated in the form of $KU = F$ as explained by 20-22 equations [39],[44]:

$$[K] = k\left[\iint_{\Omega} \frac{\partial W_i}{\partial x}\frac{\partial \emptyset}{\partial x} d\Omega + \iint_{\Omega} \frac{\partial W_i}{\partial y}\frac{\partial \emptyset}{\partial y} d\Omega\right] - \iint_{\Omega} W_i S\left(\frac{1}{\Delta t}\right) d\Omega \tag{20}$$

$$[U] = H^{n+1} \tag{21}$$

[6] Moving Least Squares

$$[F] = \iint_{\Omega} W_i S\left(\frac{H^n}{\Delta t}\right) d\Omega + Q \times \delta(x - x_w)(y - y_w) \tag{22}$$

In Eq. 20, W and $\emptyset$ represent weight and shape functions. Here, K, F and U represent the stiffness matrix, force body vector, and the unknown variables vector.

2.5. Groundwater flow equation in the unconfined aquifer

Based on the Dupouit assumption, the governed equation of groundwater flow in a transient condition is stated in Eq. 23 [48]:

$$\frac{\partial}{\partial x}\left(k_x H \frac{\partial H}{\partial x}\right) + \frac{\partial}{\partial y}\left(k_y H \frac{\partial H}{\partial y}\right) = \frac{S_y \partial H}{\partial t} + Q \times \delta(x - x_w)(y - y_w) + q \tag{23}$$

In this equation S_y denotes as specific yield.

As the following equation:

$$\frac{\partial H^2}{\partial x} = 2H\frac{\partial H}{\partial x}, \frac{\partial H^2}{\partial y} = 2H\frac{\partial H}{\partial y} \tag{24}$$

With the substitution of Eq. 24 in 23:

$$\frac{\partial}{\partial x}\left(k_x \frac{\partial H^2}{\partial x}\right) + \frac{\partial}{\partial y}\left(k_y \frac{\partial H^2}{\partial y}\right) = 2 \times \left(\frac{S_y \partial H}{\partial t} + Q \times \delta(x - x_w)(y - y_w)\right) \tag{25}$$

As the aquifer is homogeneous and isotropic ($k = k_x = k_y$):

$$k\left[\left(\frac{\partial^2 H^2}{\partial x^2}\right) + \left(\frac{\partial^2 H^2}{\partial y^2}\right)\right] = 2 \times \left(\frac{S_y \partial H}{\partial t} + Q \times \delta(x - x_w)(y - y_w)\right) \tag{26}$$

In the most discrete state of the groundwater equation, a set of linear equations $KU = F$ are obtained. In 27-29 equations, each matrix determinates [44]:

$$[K] = -2k\left[\iint_{\Omega} \frac{\partial W_i}{\partial x} H^n \frac{\partial \emptyset}{\partial x} d\Omega + \iint_{\Omega} \frac{\partial W_i}{\partial y} H^n \frac{\partial \emptyset}{\partial y} d\Omega\right] - 2\iint_{\Omega} W_i S_y \left(\frac{1}{\Delta t}\right) d\Omega. \tag{27}$$

$$[U] = H^{n+1} \tag{28}$$

$$[F] = -2\iint_{\Omega} W_i S_y \left(\frac{H^n}{\Delta t}\right) d\Omega + Q \times \delta(x - x_w)(y - y_w) \tag{29}$$

Noticed that the weight function in equations (20-22) and (27-29) is calculated with the following equation [40,42]:

$$W_i(X) = \begin{cases} \frac{2}{3} - 4\overline{r_i^2} + 4\overline{r_i^3} & \overline{r_i} \le 0.5 \\ \frac{4}{3} - 4\overline{r_i} + 4\overline{r_i^2} - \frac{4}{3}\overline{r_i^3} & 0.5 < \overline{r_i} \le 1 \\ 0 & \overline{r_i} > 1 \end{cases} \tag{30}$$

Figure 2 shows the flowchart of our work.

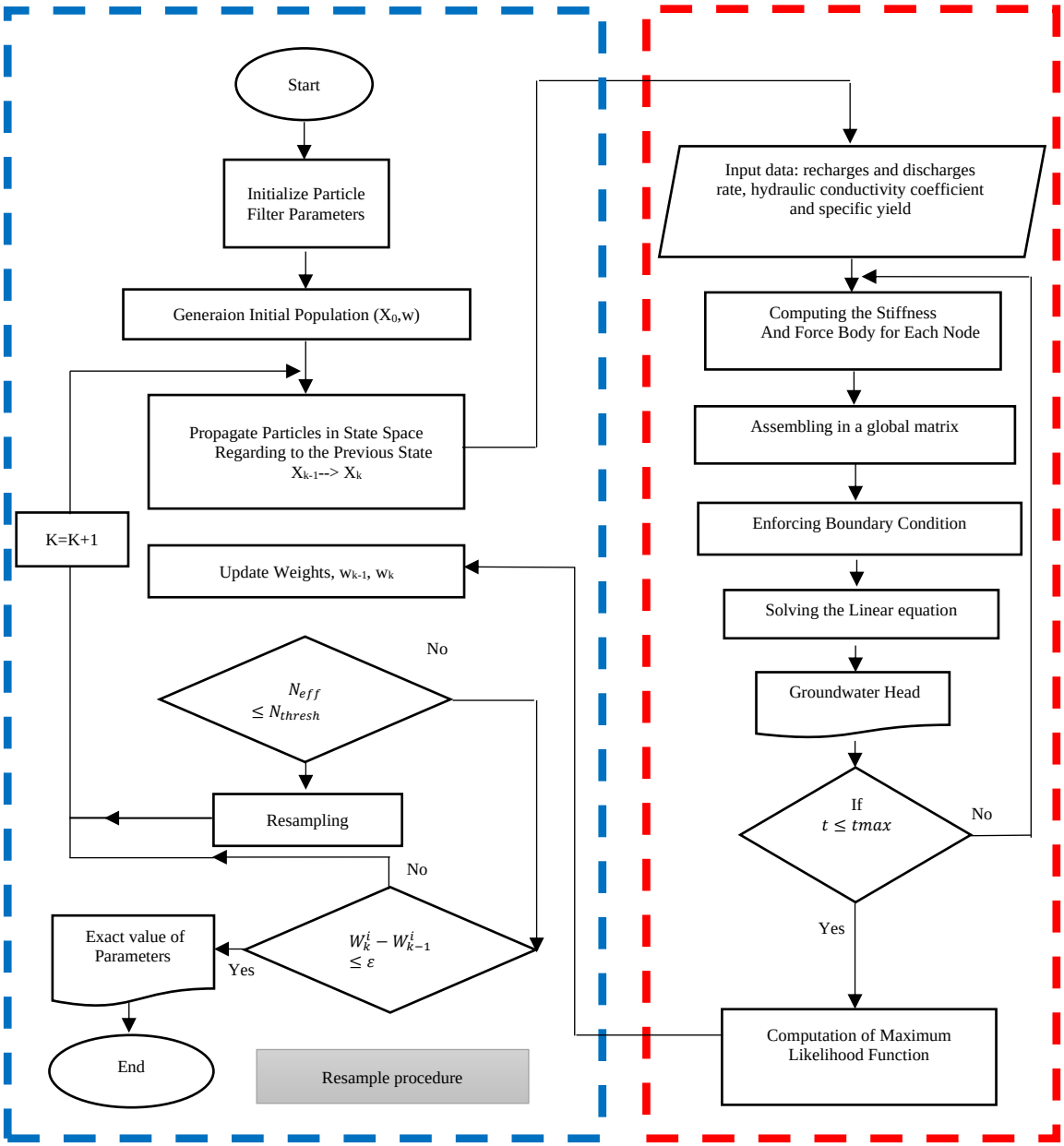


Figure 2. Flowchart of PF-MLPG-MK model

Figure 2 shows the flowchart of PF-MLPG-MK model. In the first step, the upper and lower bounds of uncertain parameters are determined. Then a set of particles generated in the state space. The dimensions of state space are equal to the number of uncertain parameters. In the first iteration (K=0), particles scattered in the state space randomly, however, in the next iterations, based on the value of maximum likelihood function, particles' location is updated. All particles have a weight value which is computed by equation 9. In the first step, this value is equal for all particles ($\frac{1}{N}$). In the next steps, based on the maximum likelihood function, new weight values are assigned to the particles. Noticed that particles with greater weight values are closer to their

exact ones.
Maximum likelihood function is calculated in the MLPG-MK model. This function is derived from [39] and is presented in the following equation:

$$w_k{}^{(i)} = w_{k-1}{}^{(i)}.\exp\left(-\frac{\frac{1}{2}(y - Sim)^2}{std^2}\right) \quad (31)$$

In Equation 31, $w_k{}^{(i)}$ and $w_{k-1}{}^{(i)}$ are the weight values in step k and k-1. y, Sim and std are the observation, simulation and standard deviation, respectively.
To prevent from degeneracy occurrence in the particle filter method, resampling technique is employed. In this situation, the particles with degenerated weight values corrected and modified. The stop condition that is defined for PF-MLPG-MK model is the difference between the current weight values and the previous weight values. If this difference is lower than a negligible value. The stop criterion is satisfied and the program is terminated.

3. Results and Discussion

PF-MLPG-MK model known as a new simulation-calibration method is investigated in three standard aquifers. In the first aquifer, hydraulic conductivity and specific yield is estimated. In the second one, two parameters e.g., transmissivity and storage coefficients are determined. In the last aquifer, the number of uncertain parameters equals to six. All of them are estimated as it is discussed in the next sections.

It must be noticed that the engaged MLPG simulation model was calibrated and verified in the real condition (field aquifer) as the following references [28],[44] and it is not discussed in this paper. The sensitivity analysis of the number of particles in PF-MLPG model is carried out as well. Three values are considered for this aim. 60, 80 and 100 particles are considered in the state space. The comparison of their results is presented in the following sections.

3.1. The first aquifer

The unconfined aquifer in Kulkarni's [49] research is used to calibrate the MLPG method herein. An unconfined aquifer is displayed in Figure 3. The dimensions of the aquifer are 3200*2800 m^2. It is both homogenous and isotropic. The eastern and western boundaries of the aquifer are constant flows with zero values, recognized as no flow boundaries and the northern and southern sides include 100 m head, as they are constant head boundaries. One observation well placed at (1000, 1000) (with blue point symbol). This aquifer has two extraction wells, located at (1400, 1400) and (1800, 1400) (red points) coordination. The discharge rate of extraction wells is 1142.85 and 1428.57 m^3/day, respectively. The initial groundwater table is considered 100 m for all nodes as well [49]. The aquifer is investigated in a transient state.

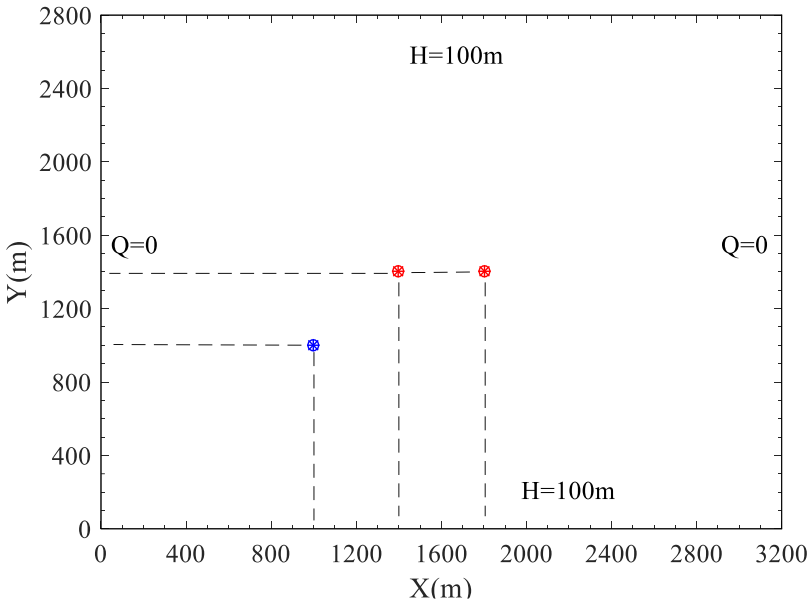


Figure 3. Representation of the first aquifer with two extraction wells and one observation well

Using the particle filter method, aquifer parameters e.g., hydraulic conductivity coefficient and specific yield coefficient are estimated. These values are 30.21 and 0.143, respectively, which are slightly different from their true values of 30 and 0.15 [49]. These differences are equal to 0.21 and 0.007. As previously mentioned, the dimensions of the state space in the particle filter algorithm are equal to the number of parameters that would be estimated. Since the two parameters of hydraulic conductivity coefficient and specific yield coefficient are estimated within this example, the state space is two-dimensional in which the first axis determines the specific yield coefficient and the second axis represents the hydraulic conductivity coefficient. The ranges considered for these coefficients are [0.001, 0.2] and [10, 100], respectively, which are specified in figure 4.

In Figure 4-a, the randomly distributed particles in the state space are presented. As time elapses and the prediction and filtration operations are implemented in the particle filter model, the particles move to a part of the state space where the particle weight is higher. Figure 4 shows the particles at the first, fourth, eighth and fifteenth stages of the model implementations.

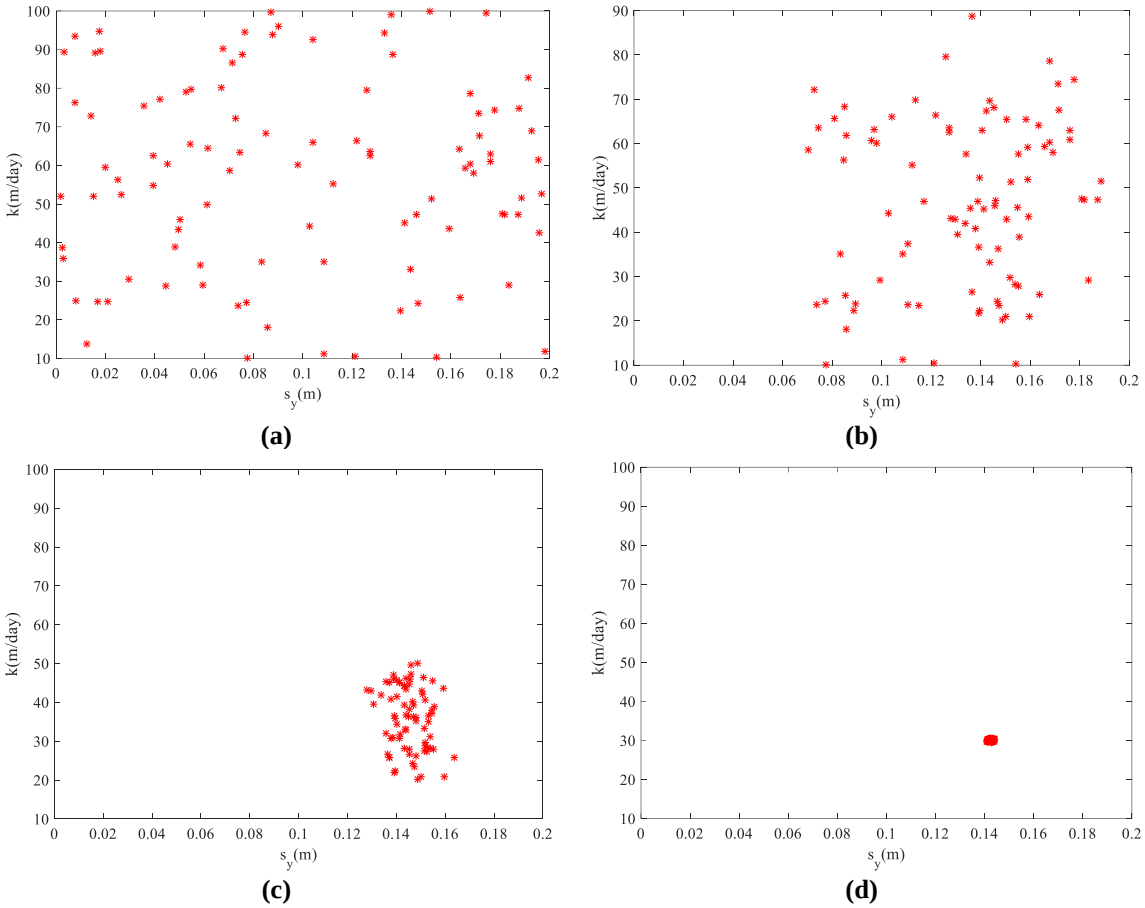


Figure 4. Simulation model a) In first stage b) In the fourth c) In eighth stage f) In fifteenth stage

Figure 4 illustrates the distribution of particles at different stages of the PF-MLPG-MK model. As previously mentioned, the horizontal axis represents the specific yield coefficient values and the vertical axis is the values of the hydraulic conductivity coefficient. As the sequence performs, the response area becomes smaller so that some particles overlap as shown in Figure 4-d. The final value is calculated based on the average state vector values at the last implementation.

In order to evaluate the accuracy of the utilized methods in groundwater flow modeling in comparison with the analytical solution, four indices of error including mean, absolute mean, root mean square, and normalized root mean square (a dimensional form of mean square root error) are used. The unit of these errors is based on the unit of the entered values. These errors are calculated using Eq. 32-35, respectively.

$$\mathrm{ME} = \frac{\sum_{t=1}^{m}\sum_{i=1}^{n}(h_{oi}^{t} - h_{si}^{t})}{n \times m} \tag{32}$$

$$\mathrm{MAE} = \frac{\sum_{t=1}^{m}\sum_{i=1}^{n}\left|h_{oi}^{t} - h_{si}^{t}\right|}{n \times m} \tag{33}$$

$$\mathrm{RMSE} = \sqrt{\frac{\sum_{t=1}^{m}\sum_{i=1}^{n}(h_{oi}^{t} - h_{si}^{t})^2}{n \times m}} \tag{34}$$

$$\mathrm{NRMSE} = \sqrt{\frac{\sum_{t=1}^{m}\sum_{i=1}^{n}(h_{oi}^{t} - h_{si}^{t})^2}{\sum_{t=1}^{m}\sum_{i=1}^{n}(h_{oi}^{t} - \overline{h_o})^2}} \tag{35}$$

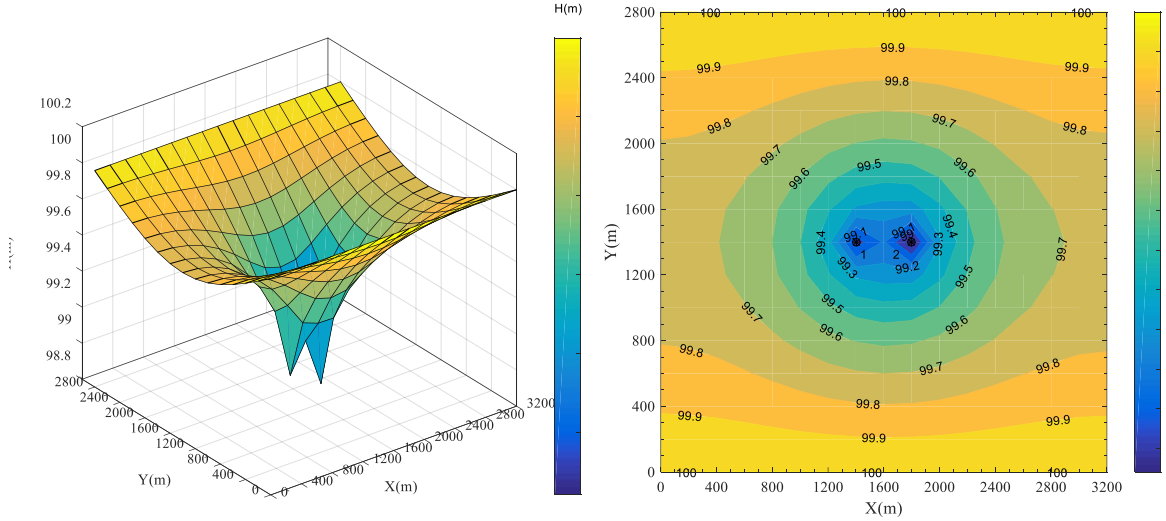
where h_{oi}^{t} ، h_{si}^{t} و $\overline{h_o}$ are the level of observed groundwater and the simulated and mean of the observed values, respectively, *n* and *m* are the number of piezometers and the number of time steps [50, 51]. Table 1 shows that the error values have been obtained from all the studied methods.

Table 1. Calculation of errors

	PF-MLPG-MK (60 particles)	PF-MLPG-MK (80 particles)	PF-MLPG-MK (100 particles)	FEM [49]	FDM [49]
Mean error (m)	-0.048	-0.035	-0.015	0.053	0.061
Mean Absolute error (m)	0.082	0.074	0.044	0.090	0.098
Root mean square error (m)	0.302	0.295	0.279	0.603	0.658
Normalized RMSE	0.128	0.119	0.114	0.248	0.270

Regarding the error values in Table 1, the error of the meshless method is much lower than the other methods, indicating the higher accuracy of this method in the modeling process of the groundwater flow. Furthermore, among the abovementioned error indices, the square root mean error is considered the main criteria [52]. This index for the meshless method is much lower than the other methods. PF-MLPG-MK for 100 particles is more accurate than 80 and 60 particles. This fact shows the role of more particles in accuracy of the model.

Figure 5 presents the groundwater head achieved from estimated parameters derived from PF-MLPG-MK model in simulation model.

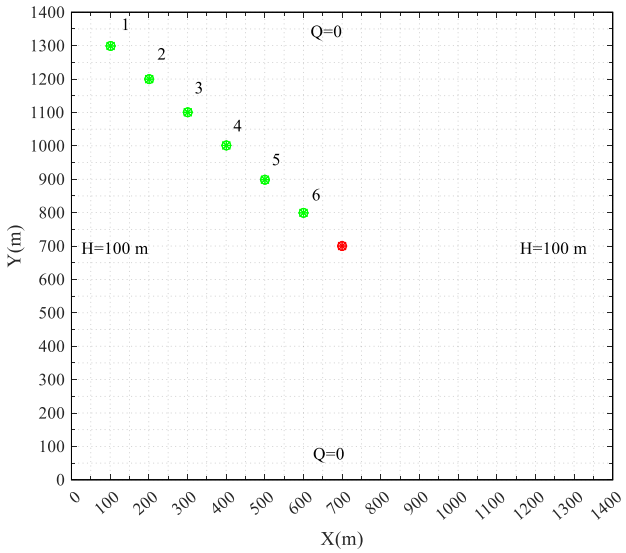


(a) **(b)**

Figure 5. The computed head by MLPG-MK a) 3D view b) 2D view

3.2. The second aquifer

A standard confined aquifer which is derived from Thomas et al. [53] is selected as the second standard case study. The aquifer is depicted in Figure 6. It is isotropic and homogenous with an area of 1400*1400 m^2. It is also surrounded by two types of boundary conditions: impervious and constant head with a value of 100 m head. As shown in Figure 6, both western and eastern edges of the aquifer have constant head boundary conditions. The aquifer initial head is equal to 100 m. An extraction well, which extracts water with a rate of 10000 m^3/day, is placed at the center of the aquifer at the coordinate of (700,700). Although this aquifer has a regular boundary (rectangular), it presents a real field aquifer with real conditions [54]. The impervious boundaries that are placed in the northern and southern boundaries of the aquifer represent mountains and the eastern and western sides of the aquifer indicate the river condition. This aquifer also has six observation wells whose positions are shown in Figure 6.



(a)

Figure 6. Representation of the second standard aquifer

With using PF-MLPG-MK method, aquifer parameters for the second aquifer are estimated. Transmissivity coefficient and storage coefficient are achieved. These values are 99.7038 and 0.001057, respectively, as their true values are 100 and 0.001 [53],[54]. The state space for this aquifer is two-dimensional as well. The horizontal axis determines the storage coefficient and the vertical axis shows the transmissivity coefficient. The ranges considered for these two parameters are [90, 150] and [0.0001, 0.005].

Figure 7 illustrates changes in locations of particles in the state space. Through the higher iteration, the particles close together. In the last iteration, almost the particles have the same coordinates. Noticed that the following figures is depicted for PF-MLPG-MK with 100 particles.

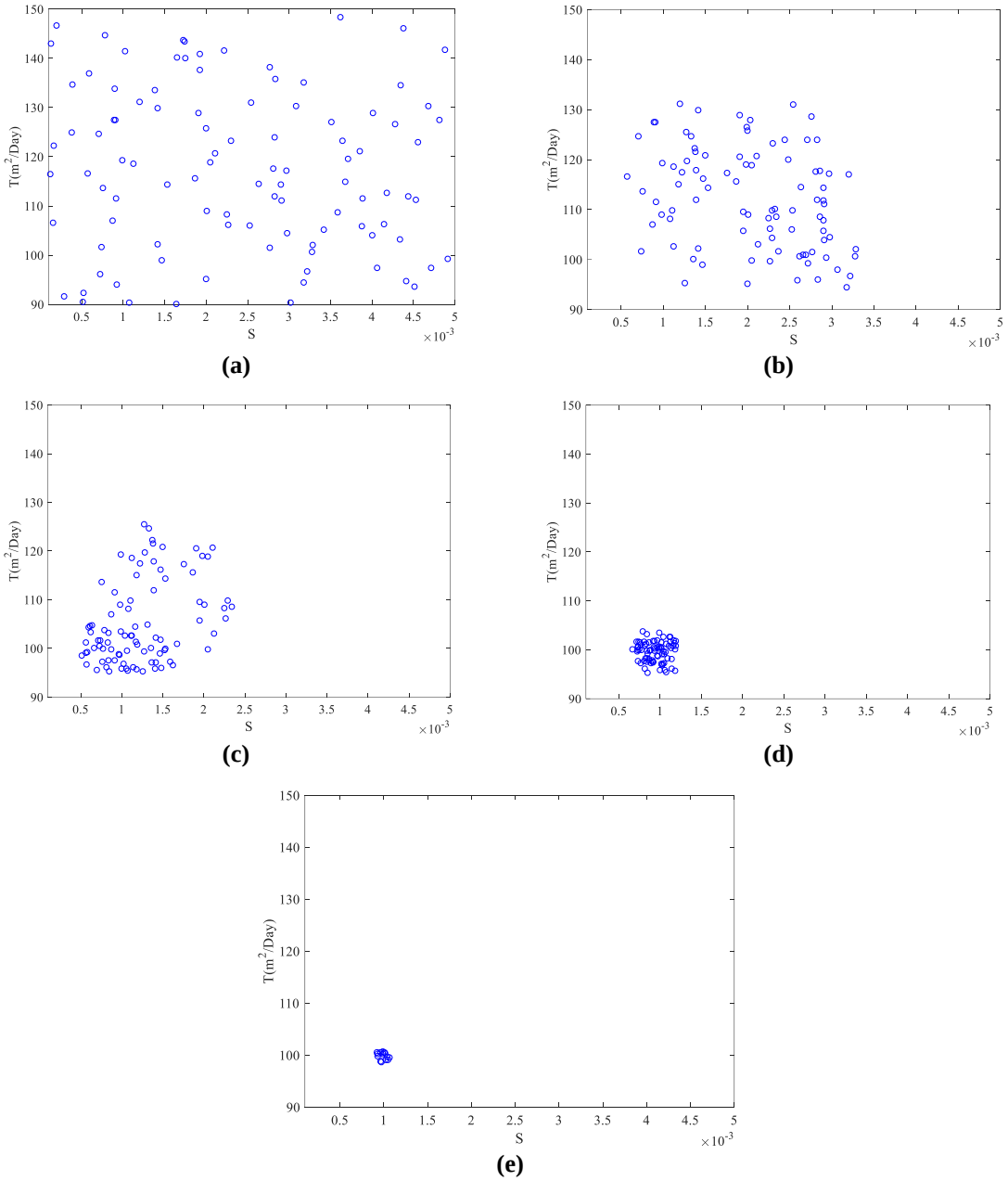


Figure 7. The convergence of particles in the second aquifer a) First stage b) Third stage c) Sixth stage d) Tenth stage. e) Thirteenth stage

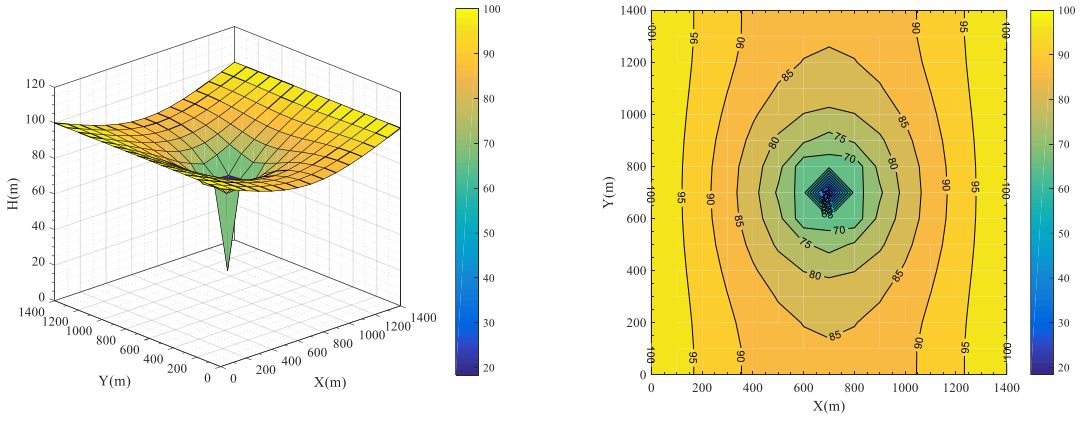
MLPG-MK simulation model is engaged in order to simulate groundwater model with the estimated parameters of PF-MLPG-MK model. In order to investigate the accuracy of the estimated parameters, the groundwater level is calculated by the results of PF-MLPG-MK and is compared with the analytical solution method and the FEM in the observation wells at points 1,2, 3, 4, 5 and 6, respectively. These results are derived from Thomas et al. [53] Table 2 shows the level of groundwater after ten days of pumping from wells. The groundwater level in the

meshless method is closer to the analytical solution than the other methods, reflecting the higher accuracy of this method. In this problem the results also show more accuracy with increasing the number of particles.

Table 2. The groundwater head computed by different methods

Well number	The observed head (m) [53]	FEM head (m) [54]	PF-MLPG-MK (m) (100 particles)	PF-MLPG-MK (80 particles)	PF-MLPG-MK (60 particles)
1	97.013	96.925	96.831		
2	93.807	93.747	93.7028		
3	90.095	90.021	89.7279		
4	85.451	85.132	85.4466		
5	78.983	78.346	78.4308		
6	67.953	67.637	67.6913		
Error calculation					
Mean error (m)		0.1494	0.14716	0.1482	0.1486
Mean Absolute error (m)		0.1494	0.14716	0.1482	0.1486
Root mean square error (m)		0.249	0.234	0.239	0.241
Normalized RMSE		0.33	0.31	0.323	0.325

Figure 8 presents the simulated groundwater head visually.



(a) **(b)**

Figure 8. The simulated groundwater head with MLPG a) 3D b)2D

3.3. The third aquifer

The standard confined aquifer, derived from Sharief et al. [55], is represented in Figure 9 and counted as a real field aquifer. The size of the domain is 1800*1000 m^2. The thickness and the storage coefficient of the aquifer are 10 m and 0.0004, respectively. The aquifer is recharged by an aquitard placed on the northern side of the aquifer recognized with an orange color. The rates of recharges are 0.00024 and 0.00012 m/day. Three extraction wells are located on (800,200),

(800,800), and (1400, 600) and extract water at a rate of 200, 500 and 700 m^3/day, respectively. There is also an injection well with the coordinates of (400,800), which injects water to the aquifer by a discharge rate of around 800 m^3/day. The aquifer is divided into three zones with different transmissivity coefficients in the x and y directions, as shown in Figure 9. Therefore, the anisotropic and heterogeneous condition is dominated. The boundary conditions in both eastern and western sides of the aquifer are constant head at a value of 100 m and 95 m. However, the northern and southern sides are impervious. There are three observation wells located at (600, 400), (1600, 400) and (1000, 600) and recognized with blue color in figure 9.

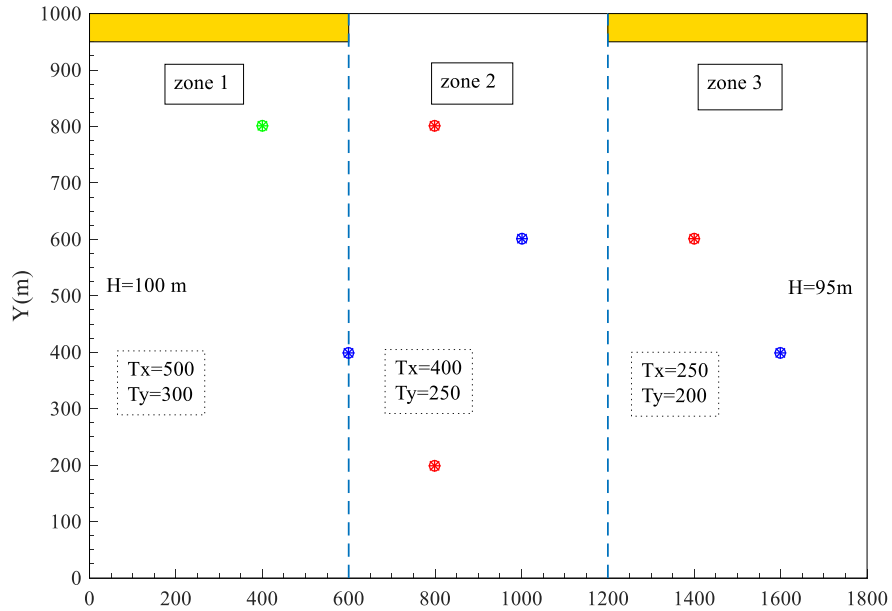


Figure 9. Representation of third standard aquifer

In this problem, there are six uncertain parameters. This aquifer has three zones with different transmissivity coefficient in x and y direction. As it is mentioned in the previous section, the dimension of state space equals to the number of uncertain parameters. Therefore, the state space is 6-dimensional and it isn't imaginable for humans [56]. The results just presented in the following table:

Table 3. Estimated aquifer parameters using PF-MLPG-MK with 100 particles

Aquifer parameters	Zone1	Zone2	Zone3
Transmissivity in x direction (m^2/day)	500.91	400.50	249.43
Transmissivity in y direction (m^2/day)	299.09	250.22	200.15

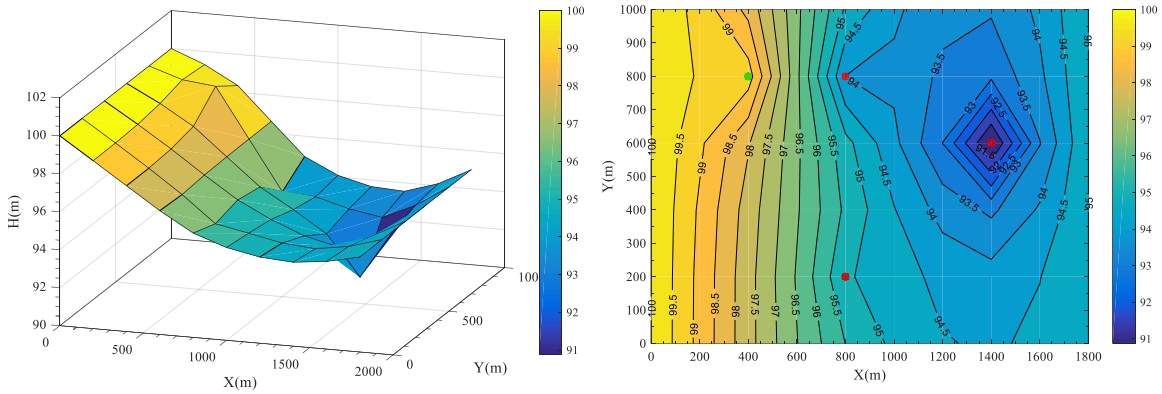
The estimated values entered to MLPG-MK simulation model and groundwater head is computed. Results of MLPG-MK method is compared with the results of the analytical solution method and the polynomial point collocation method in piezometers. The results and errors are shown in Table 4. The values presented in this table are the water level at observation wells after 10,000 days of extraction.

Table 4. Groundwater head computed by different methods in three piezometers

Piezometer number	Analytical method(m) [55]	PPCM method(m) [55]	PF-MLPG-MK(m) 100 particles	PF-MLPG-MK(m) 80 particles	PF-MLPG-MK(m) 60 particles
1	98.2	98.149	98.182		
2	97.1	96.927	97.012		
3	95.25	95.313	95.141		
Error calculation					
Mean error (m)		0.0021	0.0016	0.0018	0.0019
Mean Absolute error (m)		0.0021	0.0028	0.0029	0.0029
Root mean square error (m)		0.191	0.141	0.152	0.159

Regarding the error presented in Table 4, for each of the three piezometers, the MLPG-MK method causes more accurate responses compared to the other methods. However, in MLPG-Mk with 100 particles exhibits more accuracy than MLPG-MKs with lower particles.

Figures 10-a and 10-b show the groundwater levels in the aquifer after 10000 days. The lowering and raising of the water level in the pumping and injection wells are quite evident.



(a) **(b)**

Figure 10. a) Groundwater head in unsteady state in 3D view b) Groundwater head in unsteady state in 2D view

PF-MLPG-MK is a new coupled calibration/simulation method. As the results revealed this model can estimate the hydrodynamic parameters of aquifers regarding to its condition. Both PF and MLPG-MK method are powerful and accurate in their field. Linking these two models makes the outputs more reliable without uncertainty. The MLPG-MK groundwater simulation model, which is based on the moving kriging, is used as an effective and accurate method to model groundwater flow. The MLPG-MK method is a truly meshless method that significantly reduces all the disadvantages caused by the domain meshing and re-meshing. It is worth noting that this meshing is the most important shortcoming of the grid-dependent numerical methods such as FEM and FDM, which cause an error in the results. Another advantage of this method is that it does not need the background of a cell for numerical integration. Further, it is an easy

implementation and has better convergence and higher accuracy. In groundwater hydrology, hydraulic conductivity coefficient, transmissivity coefficient, and specific yield are among the most important aquifer parameters used for calibration. In this study, the PF-MLPG-MK method was used to predict aquifer parameters in three standard aquifers that can be considered as real aquifers. The aquifer parameters estimation was accurate enough such that they differ from the actual values of these parameters just slightly.

4. Conclusion

In this study, the particle filter method linked to the MLPG-MK approach is firstly used to estimate aquifer hydrodynamic parameters. The utilized aquifers are standard, which have real aquifer conditions and selected from previous studies. The particle filter model, which is a powerful method to estimate the dynamic models' parameters, is added to the groundwater simulation model and estimates the aquifer parameters regardless of aquifer conditions and complexity. These parameters for the first, second and third aquifers are hydraulic conductivity coefficient, specific yield and transmissivity coefficient, and storage coefficient respectively. The aquifers were arranged from a simple condition to complex one such that the third aquifer had all the conditions of a real aquifer, including rainfall, injection well, and heterogeneous and anisotropic properties. Finally, the results of the PF-MLPG-MK model show an accurate estimation of the model. For the first standard aquifer, since the true value of hydraulic conductivity and specific yield coefficients are 30 and 0.15, the predicted values are 30.21 and 0.143. In the next aquifer, transmissivity and storage coefficients are equal to 99.7038 and 0.001057 whilst their real values are 100 and 0.001, respectively. In the third standard aquifer, the estimation for the parameters also shows the same accuracy.

5. Conflict of interest

The authors declare that they have no conflict of interest.

References

1. Nayak P, SatyajiRao Y, Sudheer K, (2006). Groundwater level forcasting in a shallow aquifer using artificial, Water Resources Management, pp: 20:77-90.
2. Sreekanth PD, Sreedevi PD, Ahmed S, Geethanjali N, (2010). Comparison of FFNN and ANFIS models for estimating groundwater level, Environmental Earth Science, pp: 62:1301-1310.
3. Prinos S, Lietz A, Irvin R, Design of a real-time groundwater level monitoring network and portrayal of hydrologic data in southern Floria, US Geological Survey Report, Tallahassee, 2002.
4. Moosavi V, Vafakhah M, Shirmohammadi B, Behnia N, (2013). Awavelet-ANFIS hybrid model for groundwater level forecasting for different prediction periods, Water Resources Management, pp: 27:1301-1321.
5. Swathi, B. Eldho, T. I. (2014). Inverse Modeling Of Groundwater System Using Coupled PSO-MLPG Techniques, in International Conference on Hydroinformatics, University of New York (CUNY).
6. Chen T, Morris J, Martin E, (2004). Particle Filters for the Estimation of a State Space Model, European Symposium on Computer-Aided Process Engineering, pp: 613-618.
7. Chen T, Morris J, Martin E, (2005). Particle filters for state and parameter estimation in

batch processes, Journal of Process Control, pp: 15:665-673.
8. Kourakos G, Mantoglou A, (2012). Inverse groundwater modeling with emphasis on model parameterization, Water Resources Research, pp: 48:1-15.
9. Rai SP, (1985). Numerical determination of aquifer constants, Journal of Hydraulic Engineering, pp: 111:1110-1114.
10. Carrera J, Neuman SP, (1986). Estimation of Aquifer Parameters Under: Transient and Steady State Conditions: Maximum Likelihood Method Incorporating Prior Information, Water Resources Research, pp: 22(2):199-210.
11. YEH WWG, (1986). Review of Parameter Identification Procedures in Groundwater Hydrology: The Inverse Problem, Water Resources Research, pp: 22(2):95-108.
12. Yeh H, (1987). Theis' solution by nonlinear least-squares and finite-difference Newton's method. Groundwater, pp: 25:710-715.
13. Eppstein MJ, Dougherty DE, (1996). Simultaneous estimation of transmissivity values and zonation, Water Resources Research , pp: 32(11):3321-3336.
14. Parsad KL, Rastogi A, (2001). Estimating net aquifer recharge and zonal hydraulic conductivity values for Mahi Right Bank Canal project area, India by genetic algorithm, Journal of Hydrology, pp: 243:149-161.
15. Karahan H, Ayvaz MT, (2008). Simultaneous parameter identification of a heterogeneous aquifer system using artificial neural networks, Hydrogeology Journal, pp: 16:817-827.
16. Carrera J, Alcolea A, Medina A, Hidalgo J, (2005). Inverse problem in hydrogeology, Hydrogeology Journal, pp: 13(1):206-222.
17. Hill MC, (2006). The Practical Use of Simplicity in Developing Ground Water Models, Groundwater, pp: 44(6):775-781.
18. Fu J, Gómez-Hernández JJ, (2009). Uncertainty assessment and data worth in groundwater flow and mass transport modeling using a blocking Markov chain Monte Carlo method, Journal of Hydrology, pp: 364:328-341.
19. Ayvaz MT, Karahan H, Aral MM, (2007). Aquifer parameter and zone structure estimation using kernel-based fuzzy c-means clustering and genetic algorithm, Journal of Hydrology, pp: 343:240-253.
20. Copty NK, Trinchero P, Sanchez-Vila X, (2011). Inferring spatial distribution of the radially integrated transmissivity from pumping tests in heterogeneous confined aquifers, Water Resources Research, pp: 47(5):1-16.
21. Sahin AU, (2016). A new parameter estimation procedure for pumping test analysis using a radial basis function collocation method, Environmental Earth Science, pp: 75(200):1-13.
22. Swathi B, Eldho, TI, (2018). Aquifer parameter and zonation structure estimation using meshless local Petrov–Galerkin method and particle swarm optimization. Journal of Hydroinformatics, pp: 20(2):457-467.
23. Naderi M, (2019). Estimating confined aquifer parameters using a simple derivative-based method, Heiyon, pp: 5:1-9.
24. Thomas A, Majumdar P, Eldho TI, Rastogi AK, (2018). Simulation optimization model for aquifer parameter estimation using coupled meshfree point collocation method and cat swarm optimization. Engineering Analysis with Boundary Elements, pp: 91:60-72.
25. Thomas A, Eldho TI, Rastogi AK, Majumder P, (2019). A comparative study in aquifer parameter estimation using MFree point collocation method with evolutionary algorithms, Journal of Hydroinformatics, pp: 21(3):455-473.
26. Eryiğit M, (2021). Estimation of parameters in groundwater modelling by modified clonalg. Journal of Hydroinformatics, pp: 23(2):298-306.

27. Swathi B, Eldho TI, (2017). Groundwater flow simulation in unconfined aquifers using meshless local Petrov-Galerkin method," Engineering Analysis with Boundary Elements, pp: 48:43-52.
28. Mohtashami A, Akbarpour A, Mollazadeh M, (2017a). Development of two dimensional groundwater flow simulation model using meshless method based on MLS approximation function in unconfined aquifer in transient state, Journal of Hydroinformatics, pp: 19(5):640-652.
29. Pathania T, Bottacin-Busolin A, Rastogi AK, Eldho TI. (2019). Simulation of Groundwater Flow in an Unconfined Sloping Aquifer Using the Element-Free Galerkin Method, Water Resources Management, pp: 33:2827–2845.
30. Kambhampati, S. R.: Target/Object Tracking Using Particle Filtering, Wichita: Wichita State University, 2008.
31. Fearnhead P, Kuensch HR, (2018). Particle Filters and Data Assimilation, Annual Review of Statistics and Its Application, pp: 5(1):421-449.
32. Havangi R, (2016). Increasing consistency of particle filter using the classic method and particle swarm algorithm. Computational Intelligence in Electrical Engineering, pp: 7(2):77-88.
33. Arulampalam S, Maskell S, Gordon N, Clapp T, (2002). tutorialon particle filters for Online nonlinear/nongaussian Bayesian tracking, IEEE Transaction Signal Process, pp: 50(2):174-188.
34. Ristic B, Arulampalam, S. Gordon, N.: in Beyond Kalman Filter:Particle Filters Tracking Applicant, Boston: 1st ed, 2004.
35. Li T, Bolic M, Djuric PM, (2015). Resampling Methods for Particle Filtering: Classification, implementation and strategies, IEEE Signal Processing Magazine, pp: 32(3):70-86.
36. Choe G, Wang T, Liu F, Hyon S, Ha J, (2015). Particle filter with spline resampling and global transition model, IET Computer Vision, pp: 19(2):184-197.
37. Ruknudeen F, Asokan S, (2017). Application Particle Filter to On-Board Life Estimation of LED Lights, IEEE Photonics Journal, pp: 9(3):1-16.
38. Manoli G, Rossi M, Pasetto D, Deiana R, Ferraris S, Cassiani G, Putti M, (2015). An iterative particle filter approach for coupled hydro-geophysical inversion of a controlled infiltration experiment, Journal of Computational Physics, pp: 283:37-51.
39. Field G, Tavrisov G, Brown C, Harris A, Kreidl OP, (2016), Particle Filters to Estimate Properties of Confined Aquifers, Water Resources Management, pp: 30:3175-3189.
40. Liu G, Mesh Free Methods: Moving Beyond the Finite Element Method, Boca Raton: CRC press, 2002.
41. Porfiri M, Analysis by Meshless Local Petrov-Galerkin Method of Material Discontinuities, Pull-in Instability in MEMS, Vibrations of Cracked Beams, and Finite Deformations of Rubberlike Materials, Virginia: Virginia Polytechnic Institute and State University, 2006.
42. Liu GR, Gu YT, An introduction to Meshfree Methods and Their Programming, Singapore: Springer, 2005.
43. Atluri SN, Zhu TL, (2000). A new meshless local Petrov-Galerkin (MLPG) approach for solving problems in computational mechanics, Computational Mechanics, pp: 22:117-127.
44. Mohtashami A, Akbarpour A, Mollazadeh M, (2017b). Modeling of groundwater flow in unconfined aquifer in steady state with meshless local Petrov-Galerkin, Modares Mechanical Engineering, pp: 17(2):393-403.

45. Wang HF, Anderson MP, Introduction to groundwater modeling: finite difference and finite element methods. first ed. s.l.:Academic Press, 1995.
46. Park YC, Leap D, (2000). Modeling groundwater flow with a free and moving boundary using the element-free Galerkin (EFG) method, Geosciences Journal, pp: 4(3):243-249.
47. Wang HF, Anderson MP, Introduction to groundwater modeling: finite difference and finite element methods, first ed., Academic Press, 1995.
48. Dupouit J, Estudes Theoriques et Pratiques sur le Mouvement desEaux, Paris: Dunod, 1863.
49. Kulkarni NH, (2015). Numerical simulation of groundwater recharge from an injection well, International Journal of Water Resources and Environmental Engineering, pp: 7(5):75-83.
50. Sadeghi Tabas S, Samadi SZ, Akbarpour A, Pourreza Bilondi M, (2016), Sustainable groundwater modeling using single-and multi-objective optimization algorithms, Journal of Hydroinformatics, pp: 18(5):1-18.
51. Sadeghi-Tabas S, Akbarpour A, Pourreza-Bilondi M, Samadi S, (2016). Toward reliable calibration of aquifer hydrodynamic parameters: characterizing and optimization of arid groundwater system using swarm intelligence optimization algorithm. Arabian Journal of Geosciences, pp: 9(18):1-12.
52. Hamraz B, Akbarpour A, Bilondi MP, Sadeghi-Tabas S, (2015). On the assessment of ground water parameter uncertainty over an arid aquifer. Arabian journal of Geosciences, pp: 8(12):10759-10773.
53. Thomas, A. Eldho, T. I. Rastogi, A. K. (2012). Ground Water Flow Simulation Using Meshfree Method and Fem. in Proceedings of National Conference on Hydraulics, Water Resources, Coastal and Environmental Engineering (HYDRO-2012), Bombay, India.
54. Mategaonkar M, Eldho TI, (2011). Meshless Point Collocation Method for Ld And 2d Groundwater Flow Simulation, ISH Journal Of Hydraulic Engineering, pp: 17(1):71-87.
55. Sharief SVM, Eldho TI, Rastgoi AK, (2008). Optimal Pumping Policy for Aquifer Decontamination by Pump and Treat Method, ISH journal of Civil Engineering, pp: 14(2):1-17.
56. Alaviani F, Sedghi H, Asghari Moghaddam A, Babazadeh H, (2018). Adopting GMS–PSO Model to Reduce Groundwater Withdrawal by Integrated Water Resources Management. Environmental Research, pp: 17:619–629.

© 2021 by the authors. Licensee SCU, Ahvaz, Iran. This article is an open access article distributed under the terms and conditions of the Creative Commons Attribution 4.0 International (CC BY 4.0 license) (http://creativecommons.org/licenses/by/4.0/).